



Contents lists available at ScienceDirect

Construction and Building Materials

journal homepage: www.elsevier.com/locate/conbuildmat

Low-cycle fatigue behaviour of reinforcing bars including the effect of inelastic buckling

Mayank Tripathi^{a,*}, Rajesh P. Dhakal^a, Farhad Dashti^a, Leonardo M. Massone^b

^a Department of Civil and Natural Resources Engineering, University of Canterbury, Christchurch, New Zealand

^b Department of Civil Engineering, University of Chile, Santiago, Chile



HIGHLIGHTS

- Low-cycle fatigue life of Grade 300E and 500E reinforcing bars.
- Effect of buckling on low-cycle fatigue behaviour of reinforcing bars.
- Low-cycle fatigue model incorporating the effect of buckling.
- Effect of mean strain ratio on fatigue response of bars.

ARTICLE INFO

Article history:

Received 10 June 2018

Received in revised form 14 September 2018

Accepted 27 September 2018

Available online 6 October 2018

Keywords:

Buckling

Low-cycle fatigue

Reinforcing bars

Hysteresis

Reinforced concrete

Fatigue life

ABSTRACT

Low-cycle fatigue life of Grade 300E and 500E reinforcing bars including the effect of buckling is evaluated. Low-cycle fatigue tests are carried out on un-machined specimens subjected to constant axial strain loading with strain amplitude ranging from 1% to 5%. The experimental test observations suggest that buckling of reinforcing bars has detrimental effect on its fatigue life and increase in slenderness ratio of the reinforcing bars results in substantial reduction of their low-cycle fatigue life. Equations relating the fatigue life (i.e. number of reversals to failure) with total strain amplitude and total energy dissipated as a function of buckling parameter is proposed. Also, experimental tests are carried out to investigate the influence of mean strain ratio on low-cycle fatigue behaviour of reinforcing bars. Comparative evaluation of the fatigue life models with the results of experimental investigation shows that the proposed model can predict the fatigue life of buckled and unbuckled reinforcing bars with reasonable accuracy.

© 2018 Elsevier Ltd. All rights reserved.

1. Introduction

Reinforced concrete (RC) structures designed in compliance with current design codes are expected to resist lateral loads by undergoing large inelastic deformations at critical regions of the structure (i.e. the plastic hinge regions). The inelastic deformations in these regions are subjected to large inelastic tension-compression strain reversals, resulting in the accumulation of low-cycle fatigue damage in the reinforcement. Here, low-cycle fatigue is defined as the premature failure of reinforcing bar subjected to high strain amplitude cyclic loading in a relatively less number of cycles. This accumulation of low-cycle fatigue damage in the reinforcing bars occurs over the life span of the structure

(during seismic events and the following aftershocks) and may result in premature fracture of the reinforcing bars.

In RC structures designed to predominantly respond in flexure during a seismic event, their ultimate failure is primarily associated with either fracture of reinforcing bars due to accumulation of low-cycle fatigue damage, or buckling of reinforcing bars due to inadequate lateral restraint provided by the transverse reinforcement, or crushing of core concrete due to inadequate confinement reinforcement. Out of the flexural failure modes identified above, buckling of reinforcing bars is arguably the most common failure mode that has been observed in past earthquakes as well as in experimental tests carried out on RC walls and columns in the literature. Although researchers have extensively investigated the causes and consequences of buckling of reinforcing bars [1–8], current design methods are still unable to avoid/restrain buckling of reinforcing bars in flexurally dominated RC structures. Buckling of reinforcing bars is either accompanied by fracture of the bars due to low-cycle fatigue damage or crushing of core concrete or both, depending on the axial strain level attained in the plastic hinge regions and the

* Corresponding author.

E-mail addresses: mayank.tripathi@pg.canterbury.ac.nz (M. Tripathi), rajesh.dhakal@canterbury.ac.nz (R.P. Dhakal), farhad.dashti@canterbury.ac.nz (F. Dashti), lmassone@uchile.cl (L.M. Massone).

strain history reinforcing bars has been subjected to during the seismic event. Inelastic buckling followed by premature fracture of reinforcing bars has been observed in past experimental investigations carried out on RC columns and walls [9–12].

Reinforcement buckling inside RC structures is a more complex phenomenon than buckling of bare reinforcing bars. Recent studies have shown that multiple local parameters are known to influence the buckling response of reinforcing bars inside RC structures as compared to a bare reinforcing bars [13–16]. The buckling response of bars inside reinforced concrete members primarily depends on the resistance offered by the cover concrete and transverse reinforcement to bars against buckling. However, not much information is available on the influence of individual components (e.g. cover concrete, core concrete, tie bar stiffness, etc.) on buckling response of bars inside concrete structures. Nevertheless, the indirect way of extrapolating the results obtained from tests on bare bars is known to provide reasonably good estimation of overall response of the reinforcing bars inside reinforced concrete members. As the buckling of bars initiates while unloading from tensile strains (greater than yield strain of bars), the contribution of cracked cover concrete in restraining bar buckling is minimal. Therefore, transverse reinforcement offers the majority of the resistance against buckling of longitudinal bars. In numerical analysis of structures, the contribution of transverse reinforcement on buckling response is usually considered indirectly by evaluating the buckling length of bars and assigning the average stress-strain response of bar with the evaluated slenderness ratio.

In performance based seismic design of structures, buckling of reinforcing bars is a limit state that restricts the structure from performing its intended function and results in degradation of the overall hysteresis response (i.e. the strength, stiffness, and energy dissipation capacity) of the structure. Experimental investigations were conducted by Mander et al. [17] on ASTM A722 type II, and A615 Grade 40 deformed reinforcing bars under reversed cyclic loading with axial strains up to 6% and low-cycle fatigue models were proposed based on the total strain, plastic strain amplitude, and the dissipated energy. Brown and Kunnath [18] conducted a set of experiments on ASTM A615 reinforcing bars with varying diameters with an aim of understanding the low-cycle fatigue failure of reinforcing bars in plastic hinge regions. Based on this experimental study, fatigue life of reinforcing bars was found to be a function of bar diameter. In 2010, Hawileh et al. [19] conducted fatigue tests on ASTM A706 and A615 Grade 60 bars with strain amplitude ranging between 2% and 8%. The results of the experimental study were used to propose low-cycle fatigue material models based on total strain and plastic strain amplitudes, and the dissipated energy. Hawileh et al. [20] conducted fatigue tests on bare reinforcing bars to compare the fatigue life of different bar types and concluded that fatigue life of reinforcing bars with similar yield strength (but different bar types) can be significantly different. Hawileh et al. [21] experimentally evaluated the fatigue life of BS 460B and BS B500B reinforcing bars and concluded that yield strength of reinforcing bars influence their fatigue life. To the best of the authors' knowledge, most past research on the evaluation of low-cycle fatigue behaviour of reinforcing bars aimed to evaluate the fatigue life of bars excluding the detrimental effects of buckling. Although it has been acknowledged that buckling of reinforcing bars results in reduction of fatigue life due to weakening of material at the critical location [18], limited research has been reported in the literature on the influence of buckling on low-cycle fatigue life of reinforcing bars. Very few studies were directed to evaluate the influence of buckling on low-cycle fatigue behaviour of reinforcing bars; one exception is the study carried out by Kashani et al. [22]. Kashani et al. [22] investigated the influence of buckling on low-cycle fatigue behaviour of British smooth and ribbed reinforcing bars (BS460 and

BS500B) with varying slenderness ratios. Based on the experimental investigations, a low-cycle fatigue life model, incorporating the effect of buckling, was proposed based on total strain amplitude. Even though the proposed fatigue model incorporated the effect of buckling, the influence of yield strength of reinforcing bars and the mean strain ratio alongside buckling wasn't investigated.

In addition to the influence of buckling on low-cycle fatigue behaviour of reinforcing bars, the effect of bar strength/grade and loading history on their fatigue behaviour has also not been reported in the literature. Therefore, this paper aims to investigate the effect of inelastic buckling on low-cycle fatigue behaviour of reinforcing bars. The main objectives of the present study are; (i) to investigate the behaviour of Grade 300E and 500E deformed reinforcing bars under constant strain amplitude sinusoidal loading, with non-zero minimum strain levels; (ii) to propose low-cycle fatigue failure criteria for reinforcing bars; (iii) to evaluate the effect of inelastic buckling on low-cycle fatigue behaviour of reinforcing bars, and to develop fatigue life models incorporating the effect of bar buckling; and (iv) to investigate the effect of mean strain ratio in the presence of buckling on fatigue life of reinforcing bars.

2. Experimental test setup and results

In this study, Grade 300E and 500E deformed reinforcing bars are tested under repeated loading to evaluate their low-cycle fatigue life. These grades of reinforcing bars (with a characteristic yield strength of 300 MPa and 500 MPa respectively) are the common types of reinforcing bars used in RC structures in New Zealand. Monotonic uniaxial tension tests and low-cycle fatigue tests are carried out on 12 mm un-machined bars using a 100 kN servo-hydraulic controlled universal testing machine (UTM), with hydraulic wedge grips capable of applying both the static and fatigue loading. This machine consists of two independent hydraulic V-groove grips with each specimen being actuated independently between the hydraulic grips with a grip penetration length of 60 mm. Monotonic tension tests are carried out under displacement controlled loading with a constant loading rate of 1.0 mm/min. An axial extensometer with a gage length of 25 mm and travel range of 12.5 mm (corresponding to a maximum axial tensile strain of 50%), was mounted at the mid height of the specimen to measure the axial strains during the test. In addition to an extensometer, a potentiometer was mounted between the loading grips to measure the relative displacement of platens during the experiment. Fig. 1a shows the test setup and instrumentation used for the monotonic tension test. Monotonic tension tests were carried out on reinforcing bars with a total length of 180 mm (i.e. the length of reinforcing bar between the grips) and the axial strains were measured at the mid height of each specimen within a gage length of 25 mm. A total of three specimens for each grade of reinforcing bars are tested and the experimentally obtained average stress-strain response for Grade 300E and 500E reinforcing bars is compared in Fig. 1b, and the key characteristics of the reinforcing bars deduced from the stress-strain plots are listed in Table 1.

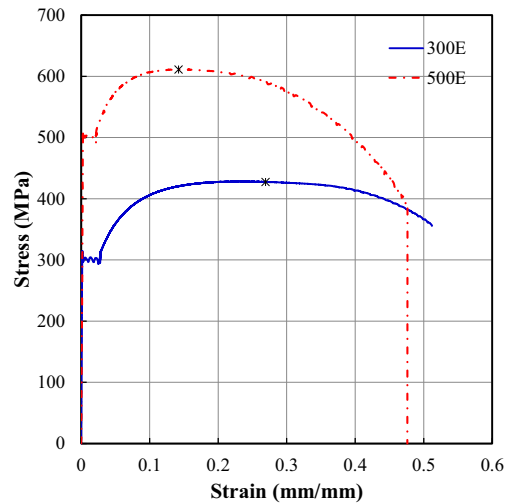
Based on the monotonic tension test results summarised in Table 1, it can be concluded that the ductility (ϵ_u/ϵ_y) of Grade 300E reinforcing bars is 3.28 times greater as compared to Grade 500E. This behaviour is expected and is associated with an increase in the carbon equivalent value (C_{eq}) of Grade 500E reinforcing bars [23]; thereby resulting in increased brittleness of the reinforcing bars.

2.1. Low-Cycle fatigue tests on reinforcing bars

The low-cycle fatigue tests are carried out on un-machined 12 mm Grade 300E and 500E reinforcing bars under constant



(a) Experimental test setup



(b) Uniaxial stress-strain response of reinforcing bars

Fig. 1. Experimental test setup and monotonic stress-strain response of reinforcing bars.

Table 1
Mechanical properties of Grade 300E and 500E reinforcing bars.

Reinforcement type	300E	500E
Yield stress f_y (MPa)	311.45	511.3
Yield strain ϵ_y	0.0015	0.0026
Modulus of elasticity E_s (MPa)	206,946	203,662
Ultimate stress f_u (MPa)	427.5	611.2
Ultimate strain ϵ_u	0.269	0.142

strain amplitude loading. The buckling of a reinforcing bar is known to depend on its yield strength (f_y) and slenderness ratio (L/D), and its behaviour can be defined by using a non-dimensional buckling parameter (λ) [24] as:

$$\lambda = \frac{L}{D} \sqrt{\frac{f_y}{100}} \quad (1)$$

Here, slenderness ratio (L/D) is the ratio of the unsupported length (i.e. buckling length, L) to diameter (D) of the bar. The effect of buckling on low-cycle fatigue behaviour of reinforcing bars is evaluated by incrementing their unsupported length (i.e. the length of the reinforcing bar between the grips representing the total length of buckling in a typical RC member) during the test. It should be noted that the buckling of reinforcing bars in RC members can span multiple tie spacing and this phenomenon is known to depend on the effective lateral restraint offered by the transverse reinforcement [25]. Therefore, the low-cycle fatigue tests are carried out on bars of different length (so that the slenderness ratio is 6, 9, 12, and 15) under constant strain amplitude loading with the total strain amplitudes of 1%, 2%, 3%, 4%, and 5% and 1%, 2%, 3%, and 4% for Grade 300E and 500E bars, respectively. The slenderness ratios are selected to represent the typical buckling length observed during tests of ductile RC structures designed and detailed according to the modern seismic codes. Sinusoidal loading waveform with frequency ranging between 0.025 and 0.125 Hz was selected, thereby resulting in a constant strain rate of 0.005 mm/mm/second for each specimen. The total length of the specimens varied between 192 mm and 300 mm (depending on the slenderness ratio of reinforcement) with each bar penetrating over a length of 60 mm in each grip. As the tested reinforcing bars were prone to buckling, instead of an extensometer a linear

potentiometer (as shown in Fig. 1a) was used to measure the axial strains (averaged over the entire length of the specimen) experienced by reinforcing bars during the test. Further, low-cycle fatigue tests with variable mean strain ratios (R) were carried out, where mean strain ratio (R) is defined as the ratio of minimum (ϵ_{\min}) to maximum (ϵ_{\max}) strain amplitude experienced by the reinforcing bars and is represented as:

$$R = \frac{\epsilon_{\min}}{\epsilon_{\max}} \quad (2)$$

Fig. 2a shows the sinusoidal loading history adopted in the experiment highlighting the key points, where T is the time period of the loading.

2.2. Low-cycle fatigue test results

The experimental test results are analysed and the number of cycles to onset of failure in the bars are determined. In a RC member, reduction in tensile capacity of the reinforcement by 50% results in significant degradation of the overall hysteresis behaviour of the member. Therefore, the onset of failure of reinforcing bars is taken when the tensile stress degrades more than 50% from the stress attained in the first cycle of the same maximum tensile strain. Fig. 2b and c illustrate the cyclic response of reinforcing bars highlighting the key points.

Figs. 3 and 4 show the hysteresis response of Grade 300E and 500E reinforcing bars with different slenderness ratio and mean strain ratio. Fig. 5 shows the fatigue failure of the buckled reinforcing bars. Figs. 3 and 4 shows that the hysteresis response of the reinforcing bars with $L/D = 6$ is symmetric in tension and compression with minimal stress degradation. Whereas, the reinforcing bars with $L/D = 15$ exhibits unsymmetrical tension-compression behaviour with significant strength degradation within the first hysteresis cycle. Furthermore, the bar with higher slenderness ratio (i.e. greater than 6) exhibits a “pinching” type of behaviour due to buckling as compared to the bars with lower slenderness ratio (typically less than 6) which exhibits a “fat” type symmetrical hysteresis loops in tension and compression. In addition to this, the results show that the buckling results in significant reduction of compressive and tensile stress capacity of the reinforcing bars. However, it should be noted that buckling not only affects the compression response of the reinforcing bars, but it also has detrimen-

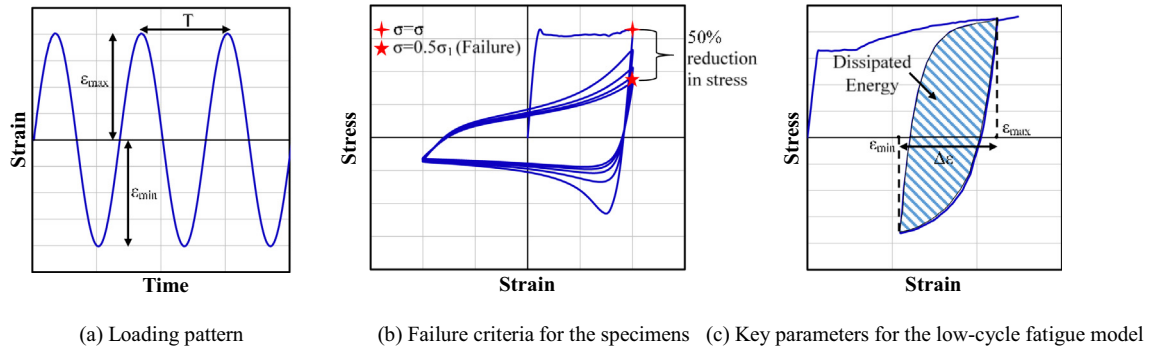


Fig. 2. Sinusoidal loading waveform, failure criteria and the key parameters.

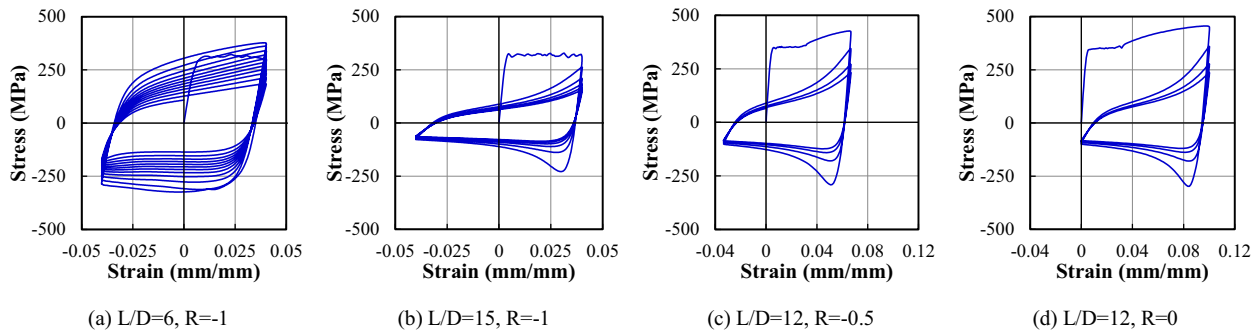


Fig. 3. Cyclic stress-strain response of Grade 300E reinforcing bars with $\epsilon_a = 0.04$ (a & b) and $\epsilon_a = 0.05$ (c&d).

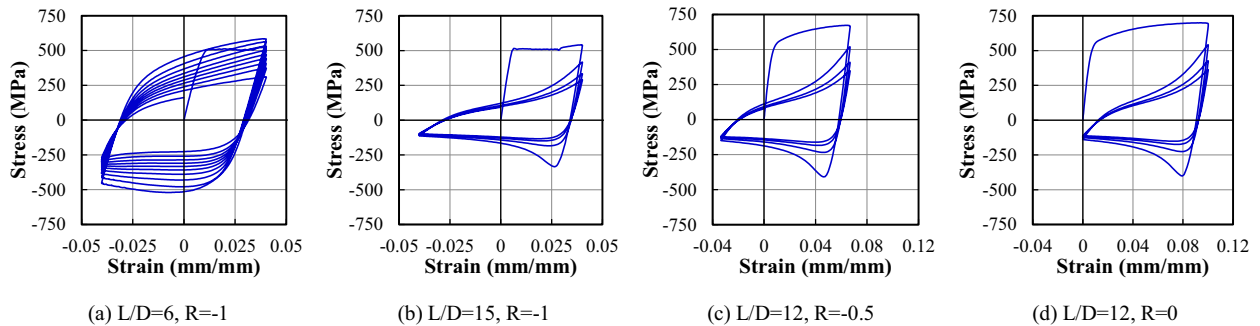


Fig. 4. Cyclic stress-strain response of Grade 500E reinforcing bars with $\epsilon_a = 0.04$ (a & b) and $\epsilon_a = 0.05$ (c&d).

tal effects on the tensile response of the bars in the subsequent strain reversals as shown in Figs. 3 and 4. This change in the type of hysteresis behaviour and degradation of the tensile stress capacity of the reinforcement is due to the presence of geometrical non-linearity in the system associated with the buckling. The results obtained through the low-cycle fatigue tests on reinforcing bars are analysed and the summary of the results are presented in Tables 2 and 3.

Based on the experimental investigations carried out on reinforcing bars, it can be concluded that low-cycle fatigue life of reinforcing bars is a function of the strain amplitude, yield strength, and slenderness ratio. Although fatigue life of a bar is also known to be influenced by its rib pattern [26], it was not considered in this study as both tested bar types (Grade 300E and 500E) had similar rib patterns. It should be noted that in all the fatigue tests, the propagation of cracks started from the inner face of the reinforcing bars at the critical location (i.e. close to mid height of the specimen), and is associated with the combined action of axial and bending stresses acting on the reinforc-

ing bars due to buckling, and is in line with the failure reported in the literature [22].

Tables 2 and 3 show that Grade 300E and 500E reinforcing bars showed different fatigue life due to difference in their yield strengths. In general, for a total strain amplitude of 0.02 or higher, the fatigue life of 500E reinforcing bars was lower compared to Grade 300E reinforcing bars. This difference in behaviour of the two bar types (Grade 300E and 500E) is mainly attributed to the increased brittleness of Grade 500E bars. Increase in brittleness expedited the fatigue damage accumulation in Grade 500E bars at large total strain amplitudes, thereby reducing their fatigue life compared to Grade 300E bars. This change in relative fatigue life of two bar types with a change in total strain amplitude is in line with findings reported in the literature. Hawileh et al. [21] conducted tests on two bar types with an average yield strength of 515 MPa and 611 MPa, and concluded that bars with high yield strength have longer fatigue life at low total strain amplitudes and smaller fatigue life at high total strain amplitudes as compared to bars with lower yield strength.



Fig. 5. Fatigue failure of buckled reinforcing bars with different slenderness ratio.

In this study, fatigue tests are also conducted with different mean strain ratios (R) with $R = -1, -0.5,$ and 0 to evaluate the influence of mean strain ratio on the low-cycle fatigue life of buckling prone reinforcing bars. For this purpose, the bars with slenderness ratios of 6 and 12 are tested again with different values of 'R'. The loading history with mean strain ratio of $R = -0.5$ and $R = 0$ is more representative of the seismic demand reinforcing bars are subjected to during an earthquake shaking (i.e. tension dominated loading with reinforcing bars being subjected to higher tensile strain compared to compressive strain). Tables 2 and 3 summarise the results of the fatigue tests with varying mean strain ratios. It should be noted that the total strain amplitude was kept constant in these cases.

Based on the test results listed in Table 2, it can be concluded that the mean strain ratio does affect the fatigue life of Grade 300E reinforcing bars. For Grade 300E reinforcing bars, at low total strain amplitudes, a change in mean strain ratio from -1 to -0.5 or 0 results in an increase in the fatigue life of the reinforcing bars. However, at larger total strain amplitudes, reinforcing bars with lower slenderness ratio (i.e. bars less prone to buckling) exhibits higher fatigue life for $R = -0.5$ and $R = 0$, compared to $R = -1$. Whereas, for reinforcing bars with a higher slenderness ratio the fatigue life reduces with tension dominated cyclic loading (i.e. fatigue life is lower for $R = -0.5$ and $R = 0$, compared to $R = -1$). For example, when the mean strain ratio (R) is changed from -1 to 0 , for a total strain amplitude (ϵ_a) of 0.05 , the fatigue life of reinforcing bars with slenderness ratio of 6 increased from 16.7 to 22, whereas the fatigue life of reinforcing bars with slenderness ratio of 12 reduced from 10 to 8.

For Grade 500E reinforcement (Table 3), at low total strain amplitude the low-cycle fatigue life reduces with tension dominated cycle. Whereas for large total strain amplitudes, it can be

Table 2 Summarized results from low-cycle fatigue tests on Grade 300E reinforcing bars.

Mean strain ratio R	Slenderness ratio L/D	Buckling parameter λ	Total strain amplitude ϵ_a	Frequency f	Max tensile strain $\epsilon_{t,max}$	Max compression strain $\epsilon_{c,max}$	Total dissipated energy ΔW_{Total}	Half cycles to failure $2N_f$
-1	6	10.59	0.01	0.125	0.010	-0.010	2159.46	838.7
			0.015	0.0833	0.015	-0.015	1087.36	214.0
			0.02	0.0625	0.020	-0.020	787.86	114.7
			0.03	0.04167	0.030	-0.030	515.31	50.0
			0.04	0.03125	0.040	-0.040	343.47	24.0
	9	15.88	0.05	0.025	0.050	-0.050	310.48	16.7
			0.01	0.125	0.010	-0.010	711.94	290.7
			0.02	0.0625	0.020	-0.020	333.85	72.0
			0.03	0.04167	0.030	-0.030	255.75	36.0
			0.04	0.03125	0.040	-0.040	207.63	22.0
	12	21.18	0.05	0.025	0.050	-0.050	173.12	14.0
			0.01	0.125	0.010	-0.010	394.23	218.0
			0.02	0.0625	0.020	-0.020	223.03	61.3
			0.03	0.04167	0.030	-0.030	151.72	27.3
			0.04	0.03125	0.040	-0.040	125.43	16.0
15	26.47	0.05	0.025	0.050	-0.050	101.11	10.0	
		0.01	0.125	0.010	-0.010	275.26	188.7	
		0.02	0.0625	0.020	-0.020	104.35	30.7	
		0.03	0.04167	0.030	-0.030	78.04	15.3	
		0.04	0.03125	0.040	-0.040	77.38	11.3	
-0.5	6	10.59	0.05	0.025	0.050	-0.050	71.26	8.0
			0.02	0.0625	0.027	-0.013	1140.37	147.0
			0.04	0.03125	0.053	-0.027	543.75	36.0
	12	21.18	0.05	0.025	0.067	-0.033	445.42	22.0
			0.02	0.0625	0.027	-0.013	335.30	85.0
			0.04	0.03125	0.053	-0.027	116.28	12.0
0	6	10.59	0.05	0.025	0.067	-0.033	102.27	8.0
			0.02	0.0625	0.040	0.000	1119.31	142.0
			0.04	0.03125	0.080	0.000	488.61	31.0
	12	21.18	0.05	0.025	0.100	0.000	430.64	22.0
			0.02	0.0625	0.040	0.000	289.22	70.0
			0.04	0.03125	0.080	0.000	112.60	10.0
			0.05	0.025	0.100	0.000	115.12	8.0

Table 3
Summarized results from low-cycle fatigue tests on Grade 500E reinforcing bars.

Mean strain ratio R	Slenderness ratio (L/D)	Buckling parameter λ	Total strain amplitude ϵ_a	Frequency f	Max tensile strain $\epsilon_{t,max}$	Max compression strain $\epsilon_{c,max}$	Total dissipated energy ΔW_{Total}	Half cycles to failure $2N_f$	
-1	6	13.57	0.02	0.0625	0.020	-0.020	1075.04	118.0	
			0.03	0.04167	0.030	-0.030	550.42	36.7	
			0.04	0.03125	0.040	-0.040	428.47	20.7	
	9	20.35	0.01	0.125	0.010	-0.010	1175.81	439.0	
			0.02	0.0625	0.020	-0.020	395.83	61.3	
			0.03	0.04167	0.030	-0.030	284.27	28.0	
	12	27.13	0.04	0.03125	0.040	-0.040	223.03	15.3	
			0.01	0.125	0.010	-0.010	515.51	204.0	
			0.02	0.0625	0.020	-0.020	243.61	47.3	
	15	33.92	0.03	0.04167	0.030	-0.030	176.83	22.0	
			0.04	0.03125	0.040	-0.040	126.66	10.7	
			0.01	0.125	0.010	-0.010	311.78	154.0	
-0.5	6	13.57	0.02	0.0625	0.027	-0.013	1069.62	113.0	
			0.04	0.03125	0.053	-0.027	387.06	17.0	
			0.05	0.025	0.067	-0.033	302.97	9.0	
	12	27.13	0.02	0.0625	0.027	-0.013	207.82	35.0	
			0.04	0.03125	0.053	-0.027	141.11	10.0	
			0.05	0.025	0.067	-0.033	130.00	7.0	
	0	6	13.57	0.02	0.0625	0.040	0.000	950.33	100.0
				0.04	0.03125	0.080	0.000	431.49	20.0
				0.05	0.025	0.100	0.000	280.42	8.0
		12	27.13	0.02	0.0625	0.040	0.000	219.54	35.0
				0.04	0.03125	0.080	0.000	154.46	10.0
				0.05	0.025	0.100	0.000	160.79	8.0

observed that the mean strain ratio (R) has little/no effect on the fatigue life of reinforcing bars regardless of its slenderness ratio (L/D). For example, when the mean strain ratio (R) is changed from -1 to 0, for a total strain amplitude (ϵ_a) of 0.02 the fatigue life of reinforcing bars with slenderness ratio (L/D) of 6 reduced from 118 to 100, whereas for a total strain amplitude (ϵ_a) of 0.04 the fatigue life of reinforcing bars with slenderness ratio (L/D) of 6 remained approximately 20. Overall, the mean strain ratio (R) has some effect on the fatigue life of the reinforcing bars, but no sustained trend can be observed. Hence, quantifying and generalising the effect of mean strain ratio on the fatigue life needs further investigation and is outside the scope of this paper. In this study, the results obtained through the fatigue tests on reinforcing bars with mean strain ratio equal to -1 are adopted for development of the low-cycle fatigue models.

3. Low-cycle fatigue behaviour of Grade 300E and 500E deformed reinforcing bars including the effect of inelastic buckling

Test results obtained from the low-cycle fatigue tests on Grade 300E and 500E bars are analysed and a fatigue life model is developed to relate the key fatigue parameters (total strain amplitude and total energy dissipated) with the number of cycles to failure. The low-cycle fatigue life models developed in the literature are based on the total strain amplitude, plastic strain amplitude and dissipated energy. Although these models are capable of predicting the fatigue life of unbuckled reinforcing bars with reasonable accuracy, they do not incorporate the detrimental effect of buckling on fatigue life. Among the above mentioned fatigue life models, strain based fatigue life models (total strain and plastic strain amplitude) are popular due to their ease in application in finite element programs. Fatigue models based on total strain amplitude are preferred over the plastic strain amplitude due to the limitation in identifying the accurate plastic strain amplitude from the experimental test results (due to the Bauchinger effect). Therefore, a low-cycle fatigue model based on total strain amplitude incorpo-

rating the effect of buckling of reinforcing bars is proposed and calibrated in this study using the test results. In addition, a fatigue model relating the dissipated total energy to the number of cycles to failure is proposed. It should be noted that the fatigue life models developed in this study are based on the experimental tests carried out on reinforcing bars under equal strain amplitude loading and therefore a suitable cycle counting algorithm [27,28] can be used to determine the cumulative fatigue damage under random loading histories.

3.1. Relationship between the total strain amplitude and low-cycle fatigue life

The low-cycle fatigue life of metals can be represented in terms of the total strain or plastic strain amplitude. Coffin Jr and Schenectady [29], and Manson [30] proposed a generalised expression for representing the fatigue life of metals:

$$\epsilon_a = \epsilon_{elastic} + \epsilon_{plastic} = \frac{\sigma'_f}{E} (2N_f)^b + \epsilon'_f (2N_f)^c \quad (3)$$

The original low-cycle fatigue model proposed by Coffin Jr and Schenectady, and Manson relates the plastic strain amplitude with the number of half cycles to failure and is represented as:

$$\epsilon_{ap} = \epsilon'_f (2N_f)^c \quad (4)$$

where, ' ϵ_{ap} ' is the plastic strain amplitude experienced by the reinforcement, and ' ϵ'_f ' and ' c ' are the fatigue life material constants to be calibrated using the experimental test results. Koh and Stephens [31] extended the low-cycle fatigue model proposed by Coffin Jr and Schenectady, and Manson and proposed a low-cycle fatigue damage model solely based on the total strain amplitude, suggesting that for most of the fatigue analysis problems the elastic strain part remains constant and can be ignored. Therefore, the low-cycle fatigue life of reinforcing bars can be evaluated using total strain amplitude given by the expression:

$$\epsilon_a = \beta (2N_f)^a \quad (5)$$

where, 'β' is the fatigue ductility coefficient and 'a' is the fatigue ductility exponent, which can be calibrated using the experimental test results, and 'N_f' is the number of cycles to the onset of failure. Fig. 6a and b show the variation of the number of half cycles to failure against the total strain amplitude for Grade 300E and 500E reinforcing bars, respectively, with different slenderness ratios. Fig. 6 clearly shows that the fatigue life reduces as the slenderness ratio is increased (i.e. as the bars become more prone to buckling). In the Fig. 6, the normalised total strain amplitude (shown in right vertical axis) is the total strain amplitude divided by the yield strain of the reinforcing bar (ε_a/ε_y).

Buckling of reinforcing bars has been extensively investigated in the literature, and it has been concluded that the buckling response of reinforcing bars can be defined using a non-dimensional buckling parameter (λ) [24]. Therefore in this study, non-linear regression analysis is carried out to correlate the fatigue life coefficients and the buckling parameter. The results obtained from low-cycle fatigue tests on reinforcing bars are fitted to the power law function and non-linear regression analysis is carried to obtain low-cycle fatigue life coefficients for different slenderness ratios. The results of regression analysis are summarised in Table 4.

A nonlinear regression analysis is conducted on the proposed fatigue life coefficients (summarised in Table 4) for different slenderness ratios and yield strengths. The results of the regression analysis indicates that the fatigue life coefficients, i.e. 'β' and 'a', are strongly correlated with the buckling parameter 'λ'. The fatigue life coefficients, 'β' and 'a', are consequently defined as a function of the buckling parameter (λ) of the reinforcing bars (i.e. the effect of inelastic buckling of reinforcing bars is taken into account) and is given by Eqs. (6) and (7). Fig. 7 shows the calibration fit of the proposed expressions with the coefficients obtained from regression analysis of the test results for Grade 300E and 500E reinforcing bars. The low-cycle fatigue life of reinforcing bars using total strain amplitude can be obtained using Eq. (5) together with these two expressions for the fatigue life coefficients. The fatigue ductility coefficient (β) and ductility exponent (a) are both found to be negatively correlated with the buckling parameter, i.e. the fatigue life coefficient reduces as the buckling parameter increases (as shown in Fig. 7).

$$\beta = \frac{-\lambda}{350} + 0.2 \tag{6}$$

Table 4

Calibration of low cycle fatigue material based on total strain amplitude for different slenderness ratio.

Reinforcement grade	Slenderness ratio L/D	Buckling parameter λ	Coefficient β	Coefficient a	R ²
300E	6	10.59	0.17	-0.45	0.99
	9	15.88	0.153	-0.454	0.97
	12	21.18	0.138	-0.458	0.99
	15	26.47	0.123	-0.462	0.93
500E	6	13.57	0.16	-0.452	0.97
	9	20.35	0.14	-0.4575	0.99
	12	27.13	0.12	-0.463	0.99
	15	33.92	0.103	-0.468	0.99

$$a = -\left(\frac{\lambda}{1200} + 0.441\right) \tag{7}$$

3.2. Relationship between hysteresis energy dissipated and low-cycle fatigue life

The hysteretic energy dissipated by the reinforcing bars under constant strain amplitude loading has been calculated by numerically integrating the area enclosed under the experimentally obtained stress-strain curve. In this study, a fatigue life model relating the total hysteresis energy dissipated before the onset of failure (ΔW_{Total}) with the number of half cycles to failure (2N_f) is proposed. The low-cycle fatigue model based on the total dissipated energy for reinforcing bars can be represented as:

$$\Delta W_{Total} = C_1(2N_f)^{\gamma_1} \tag{8}$$

where, 'C₁' and 'γ₁' are the fatigue life material coefficients that can be calibrated using the test data. Fig. 8 shows the variation of total energy dissipated for Grade 300E and 500E reinforcing bars with different slenderness ratios. The test results listed in Tables 2 and 3 and presented in Fig. 8 show that an increase in the slenderness ratio of a reinforcing bars can result in a significant drop in the total dissipated hysteresis energy due to premature failure of the bar along with the "pinching" type hysteresis response.

The total energy dissipated before the onset of failure has been calculated and a fatigue model relating the number of reversals to failure with the total energy dissipated for each

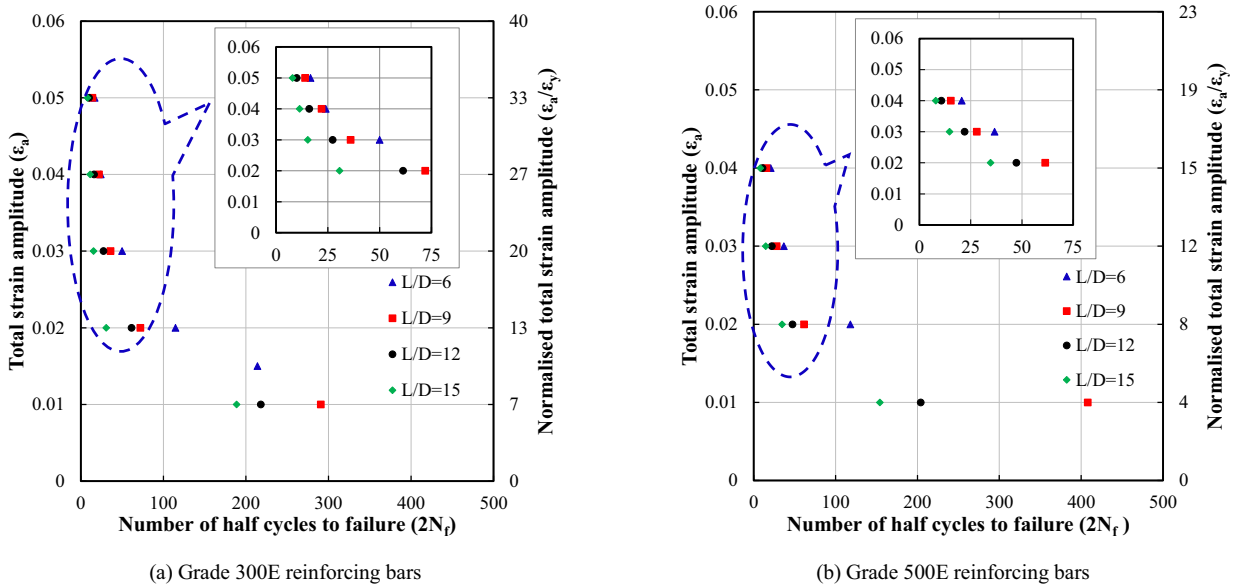


Fig. 6. Experimental data for total strain amplitude vs reversals to failure for Grade 300E and 500E reinforcing bars.

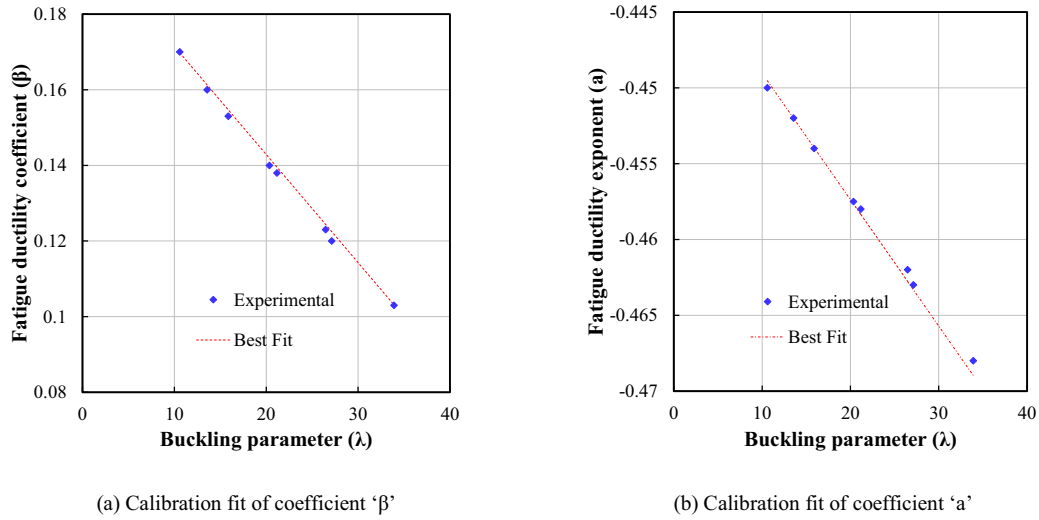


Fig. 7. Calibration of fatigue material coefficient including the effect of buckling.

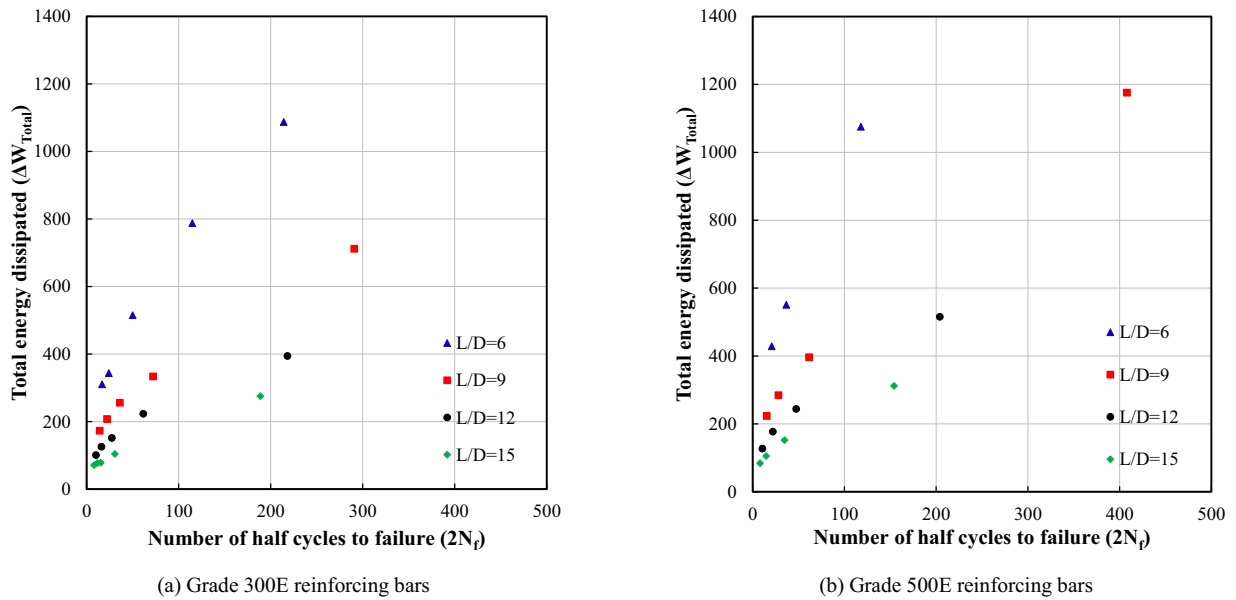


Fig. 8. Experimentally obtained total energy dissipated versus number of half cycles to failure.

Table 5
Calibration of low cycle fatigue material based on the total energy dissipated.

Reinforcement grade	Slenderness ratio L/D	Buckling parameter λ	Coefficient		R ²
			C ₁	Y ₁	
300E	6	10.59	74	0.51	0.99
	9	15.88	41.6	0.51	0.98
	12	21.18	27.5	0.51	0.97
	15	26.47	20	0.51	0.98
500E	6	13.57	86.97	0.51	0.96
	9	20.35	48.82	0.51	0.98
	12	27.13	32.41	0.51	0.98
	15	33.92	23.59	0.51	0.98

slenderness ratio is proposed. The fatigue life material constants are calibrated for each slenderness ratio of the reinforcing bars by fitting the power law function to the test results and the results of the regression analysis are summarised in Table 5. Furthermore, non-linear regression analysis of the proposed fatigue life coefficients is carried out for each slenderness ratio and a

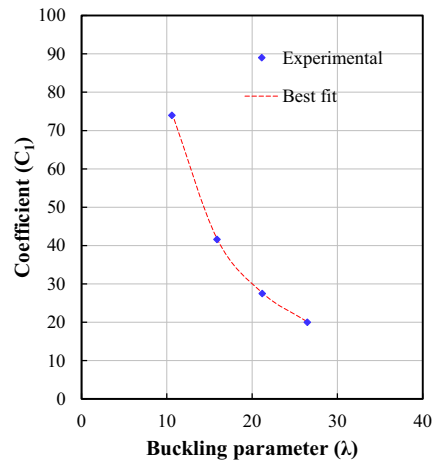


Fig. 9. Calibration of fatigue material coefficient 'C₁' including the effect of buckling.

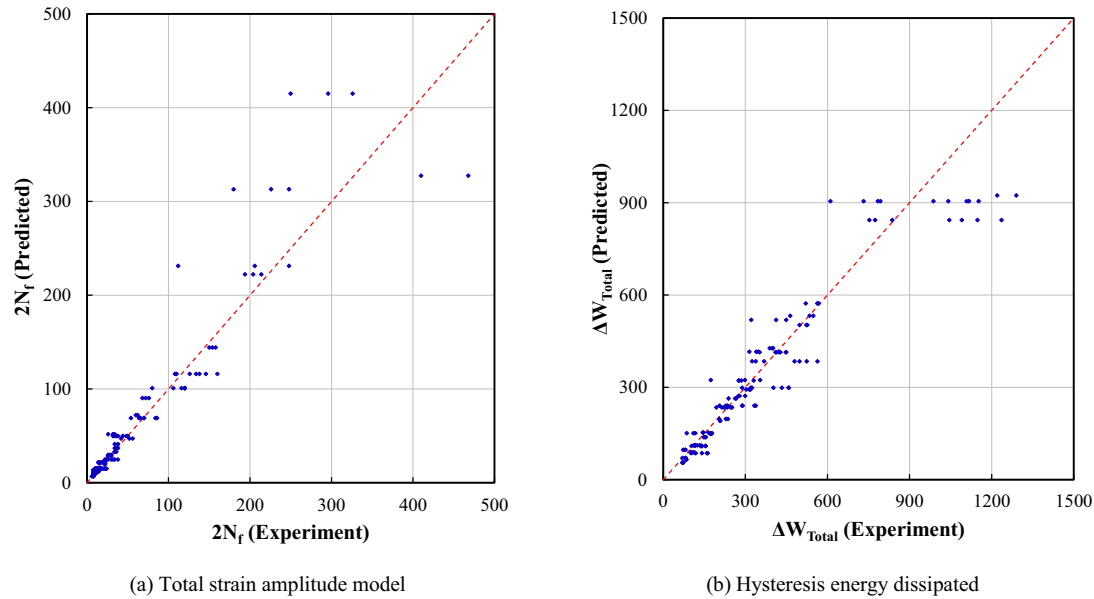


Fig. 10. Validation of the proposed fatigue life model.

unified energy based low-cycle fatigue model incorporating the effect of buckling is proposed. The total energy dissipated before the onset of failure can be evaluated using Eq. (8), where the fatigue life coefficient ' C_1 ' and ' γ_1 ' mentioned above can be calculated as:

$$C_1 = 7f_y \lambda^{-1.43} \quad (9)$$

$$\gamma_1 = 0.51 \quad (10)$$

Fig. 9 shows the calibration fit for the proposed expression with the coefficients obtained from regression analysis of test results for Grade 300E and 500E reinforcing bars.

4. Validation of the low-cycle fatigue models

To validate efficacy of the proposed fatigue life model, low-cycle fatigue tests carried out on reinforcing bars with different slenderness ratio under variable loading histories are consolidated and compared against the analytically predicted parameters (i.e. number of half cycles to failure and the total energy dissipated). Fig. 10a and 10b show the efficacy of the proposed fatigue life model for evaluating the number of half cycles to failure and hysteresis energy dissipated in presence of buckling, respectively. As shown in Fig. 10a, the proposed analytical model correlates well with the experimental results and is able to predict the number of half cycle to failure with reasonable accuracy, except for the cases with low total strain amplitudes resulting in higher fatigue life. Similarly, it can be seen in Fig. 10b that the proposed model is reliably able to predict the total hysteresis energy dissipated with reasonable accuracy. The proposed fatigue life model can be used alongside a suitable reinforcement material model to numerically simulate the cyclic behaviour of RC members with reasonable accuracy. For design or assessment application, the proposed fatigue model can be used by evaluating the number of equal amplitude strain cycles a reinforcing bar is subjected to in a structure (using the cycle counting algorithms) when the structure is exposed to design basis or actual earthquake, respectively.

5. Conclusions

In this paper, low-cycle fatigue tests on Grade 300E and 500E reinforcing bars under constant strain amplitude loading were carried out to quantify the detrimental effect of buckling on low-cycle fatigue life of reinforcing bars. The major parameters considered in the study were the grade of reinforcing bars (Grade 300E and 500E), slenderness ratio of reinforcing bars (6, 9, 12, and 15) and mean strain ratio ($R = -1.0, -0.5, 0$). The experimental results were analysed and a fatigue life model relating the total strain amplitude to the number of cycles to failure was proposed by incorporating the effect of inelastic buckling of reinforcing bars. The detrimental effect of buckling was taken into account through calibration of the fatigue life coefficients as a function of the buckling parameter (λ). Furthermore, an energy based fatigue life model relating the total energy dissipated to the number of cycles to failure has also been proposed. The major outcomes of the present study are:

1. Inelastic buckling of reinforcing bars has detrimental effect on their low-cycle fatigue life. Increase in the buckling length to bar diameter ratio of the reinforcing bars (which makes them more prone to buckling) results in decrease of their fatigue life. In other words, buckling prone reinforcing bars fail much earlier than reinforcing bars with minimal or no buckling. For instance, an increase in the buckling length of a Grade 300E bar from 6 to 15 times its diameter results in reduction of its fatigue life (number of reversals to failure) from 50 to 15 half cycles at a total strain amplitude of 0.03.
2. Inelastic buckling of a reinforcing bar results in substantial loss of its load carrying capacity both in tension and compression. As a result, in addition to adversely affecting the fatigue life of the reinforcing bars, buckling also influences the overall hysteresis behaviour of the structure. In the post-buckling phase, the peak stresses attained by a bar in the first cycle drop substantially in the subsequent cycles.
3. Yield strength of a bar significantly affects its low cycle fatigue life. For large total strain amplitudes ($\epsilon_a \geq 0.02$), low-cycle fatigue life of higher strength reinforcing bars is less than that of lower strength bars.

4. A generic fatigue life model including the effect of buckling is developed and the fatigue life coefficients used in the model are calibrated against the results of the experimental investigation. Generalized expressions for the fatigue life coefficients including the effect of bar buckling are proposed as a function of the buckling parameter (λ) (which relates the extent of buckling in terms of the yield strength (f_y) and slenderness ratio (L/D) of reinforcing bars i.e. $\lambda = \frac{L}{D} \sqrt{\frac{f_y}{100}}$).
5. Including the effect of bar buckling, the low-cycle fatigue life of reinforcing bars can be calculated as:

$$\epsilon_a = \beta(2N_f)^a$$

where,

$$\beta = \frac{-\lambda}{350} + 0.2$$

$$a = -\left(\frac{\lambda}{1200} + 0.441\right)$$

The proposed low-cycle fatigue model is found to be well corroborated with the experimental test results and can be implemented into existing finite element programs to simulate the cyclic behaviour of flexurally dominated RC structures with reasonable accuracy. Further, the proposed low-cycle fatigue model along with the relevant cycle counting algorithm can be efficiently used as a tool for assessing the remaining fatigue life of RC structures after seismic events.

Conflict of interest

None.

Acknowledgements

The authors would like to acknowledge the financial support provided by the Ministry of Business, Innovation and Employment (MBIE) and the Quake Centre at University of Canterbury for conducting the research. The testing facility provided by the Department of Mechanical Engineering, University of Canterbury for carrying out the fatigue tests on reinforcing bars is also acknowledged.

References

- [1] G. Monti, C. Nuti, Nonlinear Cyclic Behavior of Reinforcing Bars including Buckling, *J. Struct. Eng.-ASCE* 118 (12) (1992) 3268–3284.
- [2] A. Gomes, J. Appleton, Nonlinear Cyclic Stress-Strain Relationship of Reinforcing Bars including Buckling, *Eng. Struct.* 19 (10) (1997) 822–826.
- [3] M.E. Rodriguez, J.C. Botero, J. Villa, Cyclic Stress-Strain Behavior of Reinforcing Steel including Effect of Buckling, *J. Struct. Eng.-ASCE* 125 (6) (1999) 605–612.
- [4] R.P. Dhakal, K. Maekawa, Path-Dependent Cyclic Stress-Strain Relationship of Reinforcing Bar including Buckling, *Eng. Struct.* 24 (11) (2002) 1383–1396.
- [5] S.K. Kunnath, Y. Heo, J.F. Mohle, Nonlinear Uniaxial Material Model for Reinforcing Steel Bars, *J. Struct. Eng.-ASCE* 135 (4) (2009) 335–343.
- [6] L.M. Massone, D. Moroder, Buckling Modeling of Reinforcing Bars with Imperfections, *Eng. Struct.* 31 (3) (2009) 758–767.
- [7] C.R. Urmsion, J.B. Mander, Local Buckling Analysis of Longitudinal Reinforcing Bars, *J. Struct. Eng.-ASCE* 138 (1) (2012) 62–71.
- [8] M.M. Kashani, Seismic Performance of Corroded RC Bridge Piers-Development of a Multi-Mechanical Nonlinear Fibre Beam-Column Model, Civil Engineering, University of Bristol, 2014.
- [9] A. El-Bahy, S.K. Kunnath, W.C. Stone, A.W. Taylor, Cumulative Seismic Damage of Circular Bridge Columns: Benchmark and Low-Cycle Fatigue Tests, *ACI Struct. J.* 96 (1999) 633–641.
- [10] D. Lehman, J. Moehle, S. Mahin, A. Calderone, L. Henry, Experimental Evaluation of the Seismic Performance of Reinforced Concrete Bridge Columns, *J. Struct. Eng.-ASCE* 130 (6) (2004) 869–879.
- [11] A. Dazio, K. Beyer, H. Bachmann, Quasi-Static Cyclic Tests and Plastic Hinge Analysis of RC Structural Walls, *Eng. Struct.* 31 (7) (2009) 1556–1571.
- [12] F. Dashti, R.P. Dhakal, S. Pampanin, Tests on Slender Ductile Structural Walls Designed According to New Zealand Standard, *Bulletin of the New Zealand Society for Earthquake Engineering* 50 (4) (2017) 504–516.
- [13] Z. Zong, Uniaxial Material Model incorporating Buckling for Reinforcing Bars in Concrete Structures subjected to Seismic Loads, Civil and Environmental Engineering, University of California Davis, California, 2010.
- [14] M.M. Kashani, L.N. Lowes, A.J. Crewe, N.A. Alexander, Nonlinear Fibre Element Modelling of RC Bridge Piers considering Inelastic Buckling of Reinforcement, *Eng. Struct.* 116 (2016) 163–177.
- [15] M.M. Kashani, M.R. Salami, K. Goda, N.A. Alexander, Non-linear Flexural Behaviour of RC Columns including Bar Buckling and Fatigue Degradation, *Mag. Concr. Res.* 70 (5) (2017) 231–247.
- [16] A. Nojavan, A.E. Schultz, S.-H. Chao, Analytical study of In-plane Buckling of Longitudinal Bars in Reinforced Concrete Columns under Extreme Earthquake Loading, *Eng. Struct.* 134 (2017) 48–60.
- [17] J.B. Mander, F.D. Panthaki, A. Kasalanati, Low-Cycle Fatigue Behavior of Reinforcing Steel, *J. Mater. Civ. Eng.* 6 (4) (1994) 453–468.
- [18] J. Brown, S.K. Kunnath, Low-Cycle Fatigue Failure of Reinforcing Steel Bars, *ACI Mater. J.* 101 (6) (2004) 457–466.
- [19] R. Hawileh, A. Rahman, H. Tabatabai, Evaluation of the Low-Cycle Fatigue Life in ASTM A706 and A615 Grade 60 Steel Reinforcing Bars, *J. Mater. Civ. Eng.* 22 (1) (2010) 65–76.
- [20] R. Hawileh, A. Tabatabai, A. Abu-Obeidah, J. Balloni, A. Rahman, Evaluation of the Low-Cycle Fatigue Life in Seven Steel Bar Types, *J. Mater. Civ. Eng.* 28 (5) (2015) 06015015.
- [21] R.A. Hawileh, J.A. Abdalla, F. Oudah, K. Abdelrahman, Low-Cycle Fatigue Life Behaviour of BS 460B and BS B500B Steel Reinforcing Bars, *Fatigue Fract. Eng. Mater. Struct.* 33 (7) (2010) 397–407.
- [22] M.M. Kashani, A.K. Barmi, V.S. Malinova, Influence of Inelastic Buckling on Low-Cycle Fatigue Degradation of Reinforcing Bars, *Constr. Build. Mater.* 94 (2015) 644–655.
- [23] AS/NZS4671-2001, Steel, Reinforcing Materials, Standards New Zealand (2001).
- [24] R.P. Dhakal, K. Maekawa, Modeling for Postyield Buckling of Reinforcement, *J. Struct. Eng.-ASCE* 128 (9) (2002) 1139–1147.
- [25] R.P. Dhakal, K. Maekawa, Reinforcement Stability and Fracture of Cover Concrete in Reinforced Concrete Members, *J. Struct. Eng.-ASCE* 128 (10) (2002) 1253–1262.
- [26] T. Helgason, J. Hanson, N. Somes, W. Corley, E. Hognestad, Fatigue Strength of High-yield Reinforcing Bars, NCHRP Report (164) (1976).
- [27] M.A. Miner, Cumulative Damage in Fatigue, *J. Appl. Mech.* 12 (1945) A159–A164.
- [28] M.T. Suidan, R.A. Eubanks, Cumulative Fatigue Damage in Seismic Structures, *J. Struct. Div.-ASCE* 99 (1973) 923–941.
- [29] L.F. Coffin Jr, N.Y. Schenectady, A Study of the effects of Cyclic Thermal Stresses on a Ductile Metal, *Trans. ASME* 76 (1954) 931–950.
- [30] S.S. Manson, Behavior of Materials under conditions of Thermal Stress, Heat Transfer Symposium, University of Michigan Engineering Research Institute, Ann Arbor, Michigan, 1953.
- [31] S. Koh, R. Stephens, Mean Stress effects on Low Cycle Fatigue for a High Strength Steel, *Fatigue Fract. Eng. Mater. Struct.* 14 (4) (1991) 413–428.